Synthesis, Crystal Structures and Physical Properties of μ-Oxo-μ-carboxylato-diiron(III) Complexes with Tripodal Polybenzimidazole Ligands containing Distinct Iron Sites†

Shuangxi Wang,*[a] Qinhui Luo,*[a] Ximeng Wang,[a] Liufang Wang[b,c] and Kaibei Yu[d]

[a] *Co-ordination Chemistry Institute, Nanjing University, Nanjing 210093, China*

[b] *State Key Laboratory for Oxo Synthesis and Selective Oxidation, Lanzhou Institute of Chemical Physics, Academia Sinica, Lanzhou 730000, China*

[c] *National Laboratory of Applied Organic Chemistry, Lanzhou University, Lanzhou 730000, China*

[d] *Chengdu Centre of Analysis and Measurement, Academia Sinica, Chengdu 610005, China*

μ-Oxo-μ-carboxylato-diiron complexes $[Fe_2O(O_2CR)L_2]X_3$ (R = Me or Ph, X = ClO_4 or NO_3) with the tripodal polybenzimidazole tris[(benzimidazol-2-yl)methyl]amine (L^1), tris[(*N*-methylbenzimidazol-2-yl)methyl]amine (L^2) and tris[(*N*-ethylbenzimidazol-2-yl)methyl]amine (L^3) have been synthesized and characterized by elemental analysis, IR, electronic, resonance-Raman and ^1H NMR spectroscopies and cyclic voltammetry. The crystal structures of $[Fe_2O(O_2CMe)L^2_2][ClO_4]_3H_2O·3MeCN$ and $[Fe_2O(O_2CPh)L^2_2][ClO_4]_3·H_2O·2MeCN$ have been determined. They show that the complexes contain two distinct iron sites. At one the benzimidazole nitrogen atom is *trans* to the oxo-bridge, while at the other the tertiary amine nitrogen atom is *trans* to the oxo-bridge. That this solid-state structure persists in solution was confirmed by ^1H NMR spectroscopy. The asymmetry is manifested in the resonance Raman spectra as an enhancement of ν_{asym}(Fe–O–Fe) and a large intensity ratio (I_{asym}/I_{sym} 0.19–0.26:1) of ν_{asym}(Fe–O–Fe) to ν_{sym}(Fe–O–Fe). The first complex exhibits strongly antiferromagnetic exchange with a J value of -108.22 cm^{-1}. The Mössbauer spectra of these two complexes and of $[Fe_2O(O_2CMe)L^3_2][ClO_4]_3·0.5H_2O$ have been recorded. The electrochemical results show that the complexes exhibit completely irreversible redox behaviour which is different from that found in μ-oxo-diiron proteins.

The chemistry of the μ-oxo-diiron(III) core is well developed and continues to be studied because of the growing awareness of the existence of this unit in non-haem iron proteins, such as haemerythrin, the R_2 protein of ribonucleotide reductase, the hydroxylase component of methane monooxygenase and purple acid phosphatase.[1] The first three of these proteins have been characterized extensively by various spectroscopic methods as well as X-ray crystallography. Methaemerythrin, R_2 and methane monooxygenase in their diiron(III) forms contain a μ-oxo-bis(μ-carboxylato)-, μ-oxo-μ-carboxylato- and a μ-hydroxo-bis(μ-carboxylato)-diiron(III) core respectively.[2–4] An important feature for these proteins is the asymmetry of the μ-oxo- or μ-hydroxo-diiron motif. Haemerythrin has two dissimilar iron sites, one five- and the other six-co-ordinate, and the sixth site in the former being involved in its biological function of dioxygen carrier.[1a] In addition, the crystal structure results demonstrated unequivocally that the diiron centres in R_2 and methane monooxygenase have different co-ordination environments.[3,4] Moreover, it is clear that a variety of uniquely biological functions for the metalloproteins are often related to the novel geometries around metal active centres, such as high distortion and asymmetry. However, most previous synthetic μ-oxo-diiron complexes are symmetric and remarkably unreactive species.[5–9] Only a limited number of asymmetric μ-oxo-diiron complexes have been reported.[10–13] Thus, the challenge remains for synthetic inorganic chemists to design molecules which can mimic the asymmetry and ultimately the biological functions found in these diiron proteins.

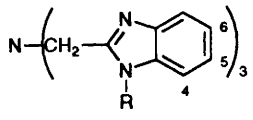

	R
L^1	H
L^2	Me
L^3	Et

Recently we have been interested in the development of the co-ordination chemistry of metal complexes with ligands containing benzimidazole units.[14] We have synthesized and investigated asymmetric μ-oxo-μ-carboxylato-diiron(III) complexes where the two iron sites are inequivalent, using the tripodal ligands tris[(benzimidazol-2-yl)methyl]amine (L^1),[15] tris[(*N*-methylbenzimidazol-2-yl)methyl]amine (L^2) and tris-[(*N*-ethylbenzimidazol-2-yl)methyl]amine (L^3). In this paper we report their structures and physical properties.

Experimental

The tripodal compounds L^1–L^3 were synthesized by following published methods.[16] All other chemicals were commercially available and used without further purification. Acetonitrile for electrochemical experiments was purified before use by standard methods. **CAUTION**: the perchlorate salts used in this study are potentially explosive and should be handled with care.

Synthesis of the Complexes.—The complexes were all synthesized in a similar manner. A typical preparation is as follows: L^2 (105 mg, 0.24 mmol) in methanol (20 cm^3) was

† *Supplementary data available:* see Instructions for Authors, *J. Chem. Soc., Dalton Trans.*, 1995, Issue 1, pp. xxv–xxx.

Non-SI unit employed: $\mu_B \approx 9.27 \times 10^{-24}$ J T^{-1}, emu = SI × $10^6/4\pi$.

treated with $Fe(ClO_4)_3 \cdot 9H_2O$ (123 mg, 0.24 mmol) in methanol (3 cm^3). To the resultant red solution was added $NaO_2CMe \cdot 3H_2O$ (55 mg, 0.4 mmol) with stirring at room temperature. The solution turned green-brown in a few minutes, followed by precipitation of the complex as a green powder. After stirring for several hours the green precipitate was filtered off and recrystallized by vapour diffusion of diethyl ether into a filtered acetonitrile solution of the complex. The complexes $[Fe_2O(O_2CPh)L_2][ClO_4]_3 \cdot nH_2O$ (L = L^1–L^3) were obtained by the same above procedure except that NaO_2CPh was used instead of $NaO_2CMe \cdot 3H_2O$: $[Fe_2O(O_2CMe)L^1{}_2][ClO_4]_3 \cdot 3H_2O$ **1** (Found: C, 44.10; H, 3.75; N, 14.05. $C_{50}H_{51}Cl_3Fe_2N_{14}O_{18}$ requires C, 44.35, H, 3.75; N, 14.50%); $[Fe_2O(O_2CPh)L^1{}_2][ClO_4]_3 \cdot 2H_2O$ **2** (Found: C, 47.65; H, 3.60; N, 13.90. $C_{55}H_{51}Cl_3Fe_2N_{14}O_{17}$ requires C, 47.25; H, 3.65; N, 14.05%); $[Fe_2O(O_2CMe)L^2{}_2][NO_3]_3 \cdot 4H_2O$ **3** (Found: C, 49.90; H, 4.55; N, 17.65. $C_{56}H_{65}Fe_2N_{17}O_{16}$ requires C, 50.05; H, 4.85; N, 17.20%); $[Fe_2O(O_2CMe)L^2{}_2][ClO_4]_3 \cdot H_2O$ **4** (Found: C, 47.55; H, 4.30; N, 13.45. $C_{56}H_{59}Cl_3Fe_2N_{14}O_{16}$ requires C, 47.95; H, 4.20; N, 14.00%); $[Fe_2O(O_2CPh)L^2{}_2][ClO_4]_3 \cdot H_2O$ **5** (Found: C, 50.35; H, 4.25; N, 13.10. $C_{61}H_{61}Cl_3Fe_2N_{14}O_{16}$ requires C, 50.00; H, 4.15; N, 13.40%); $[Fe_2O(O_2CMe)L^3{}_2][ClO_4]_3 \cdot 0.5H_2O$ **6** (Found: C, 50.00; H, 4.65; N, 12.95. $C_{62}H_{70}Cl_3Fe_2N_{14}O_{15.5}$ requires C, 50.40; H, 4.75; N, 13.25%); $[Fe_2O(O_2CPh)L^3{}_2][ClO_4]_3 \cdot H_2O$ **7** (Found: C, 51.65; H, 4.95; N, 12.30. $C_{67}H_{73}Cl_3Fe_2N_{14}O_{16}$ requires C, 51.95; H, 4.70; N, 12.65%).

Physical Measurements.—Microanalyses (C, H, N) were performed on a Carblo-Erba 1106 elemental analyser. The IR spectra were recorded on a Nicolet-170 SX FT-IR spectrophotometer as KBr discs in the range 4000–200 cm^{-1}, ^1H NMR spectra using a Bruker AM 400 spectrometer. Raman spectra were recorded on a 1403 laser spectrophotometer with 457.9 nm excitation. The scattering intensities for solid samples were quantitatively measured by a reported method.[17] Electronic spectra were recorded on a UV-240 spectrophotometer in the 190–900 nm region using acetonitrile solutions. Electrochemical studies were performed with a BAS 100 electrochemical analyser at ambient temperature in acetonitrile by using a three-electrode system consisting of a glass–carbon working electrode, a platinum auxiliary electrode and saturated calomel reference electrode (SCE) with 0.1 mol dm^{-3} tetrabutylammonium perchlorate as the supporting electrolyte.

Magnetic Studies.—Magnetic susceptibility measurements were carried out using a CAHN-200 Faraday-type magnetometer operating at 50 kG (5T) in the range 3–300 K. A powdered sample of complex **4** (56 mg) was placed in a Kelf bucket which had been calibrated independently. Diamagnetic contributions were evaluated using Pascal's constants.[18] The data were modelled by using the Heisenberg–Dirac–van Vleck equation (1) for magnetic coupling between two iron(III)

$$\chi_{calc} = P\frac{g^2S(S+1)N\beta^2}{3kT} + (1-P)\frac{Ng^2\beta^2}{kT} \times \frac{2e^{2x} + 10e^{6x} + 28e^{12x} + 60e^{20x} + 110e^{30x}}{1 + 3e^{2x} + 5e^{6x} + 7e^{12x} + 9e^{20x} + 11e^{30x}} + N_\alpha \quad (1)$$

ions, derived from the general isotropic exchange Hamiltonian $H_0 = -2JS_1S_2$ where $S_1 = S_2 = \frac{5}{2}$. Here N, k and β have their usual meanings, $x = J/kT$ and P = mole percentage of paramagnetic impurity. The temperature independent paramagnetic susceptibility term (N_α) results from the mixing of non-thermally populated wavefunctions of low-lying excited states into the ground-state wavefunction.[18] The value minimized was $R = \Sigma(\chi_{exptl} - \chi_{calc})^2/n\Sigma(\chi_{exptl})^2$ where n is the number of data (40).

Mössbauer Studies.—Mössbauer spectra were obtained at room temperature using a Halder MR −351 type spectrometer. A 10 mCi (3.7×10^8 Bq) ^{57}Co (Rh) source was used. The spectrometer was calibrated with respect to standard stainless steel at room temperature. All the spectra were fitted by Lorentzian line shapes using least-squares methods.

Crystal Structure Determinations.—Single crystals of complexes **4**·3MeCN and **5**·2MeCN were obtained by slow vapour diffusion of ether into acetonitrile solutions of the complexes. Large single crystals with dimensions 0.40 × 0.50 × 0.50 and 0.20 × 0.56 × 0.60 mm respectively were sealed in Lindeman capillaries containing mother-liquor to prevent solvent loss. The crystal data were collected on a R3M/E four-circle diffractometer with a graphite monochromator using a Mo-Kα radiation (λ = 0.710 73 Å). The unit-cell dimensions were determined by centring 25 reflections with $7 \leqslant 2\theta \leqslant 24°$ (**4**·3MeCN) and $8 \leqslant 2\theta \leqslant 24°$ (**5**·2MeCN) and refined by least squares. Intensities were measured with a θ–2θ scan mode and a scan rate of 8° min^{-1}. Details of the data collection and processing are given in Table 1. The five standard reflections monitored periodically during data collection varied in intensities by less than 3.2 and 2.9% for **4**·3MeCN and **5**·2MeCN respectively. The data were corrected for Lorentz and polarization effects. An absorption correction was applied using φ-scan data.[19]

Solution and refinement. The structures were solved by direct methods and successive Fourier-difference syntheses and refined by full-matrix least-squares methods. The weighting scheme was $w = [\sigma^2(F) + 0.000\,12F^2]^{-1}\{1 - \exp - 5\,[(\sin\theta)/\lambda]^2\}$. The hydrogen atoms were generated geometrically and included isotropically in the structure-factor calculations, but not refined. The largest electron density peaks in the difference maps were less than 0.734 and 1.241 e $Å^{-3}$ respectively, the latter being in the vicinity of the perchlorate anions.

Atomic scattering factors were taken from ref. 20. All calculations were performed with the SHELXTL program.[21]

Additional material available from the Cambridge Crystallographic Data Centre comprises H-atom coordinates, thermal parameters and remaining bond lengths and angles.

Results and Discussion

We have investigated the iron(III) co-ordination chemistry of the tetradentate tripodal compound tris[(benzimidazol-2-yl)-methyl]amine (L^1) and its 1-methyl (L^2) and 1-ethyl (L^3) derivatives to model the active sites of μ-oxo-diiron proteins. The desired doubly bridged μ-oxo-μ-carboxylato-diiron(III) complexes **1**–**7** were obtained in 70–85% yields by reactions of L^1–L^3 with $Fe(ClO_4)_3 \cdot 9H_2O$ or $Fe(NO_3)_3 \cdot 9H_2O$ in the presence of an excess of sodium acetate or sodium benzoate. The present synthetic method is different from that reported by Nishida *et al.*[15a] where the basic iron(III) acetate was used as a starting material. In our method, the presence of an excess of NaO_2CPh or NaO_2CMe appears to be necessary for the formation of the μ-oxo-μ-carboxylato-diiron core, when using $Fe(ClO_4)_3 \cdot 9H_2O$ or $Fe(NO_3)_3 \cdot 9H_2O$ as the metal source. No analytically pure complexes were obtained if the stoichiometric amounts of the benzoate or acetate were used. This may be due to the following reasons: (*i*) the presence of an excess can keep the reaction system sufficiently basic for the formation of the oxo-bridged diiron core; (*ii*) it also suppresses exchange of the bridging carboxylate groups with other anions such as NO_3^-, ClO_4^-, solvent or crystal water molecules which favours the formation of the μ-oxo-μ-carboxylato-diiron core; the lability of the carboxylate, bridges in other μ-oxo-μ-carboxylato-diiron complexes has been observed.[10,22–25] An attempt to synthesize μ-hydroxo-μ-carboxylato-diiron complexes with these ligands using Lippard's method[5b] was unsuccessful. X-Ray quality crystals of **4** and **5** were obtained by the slow diffusion method.

Table 1 Crystallographic data for complexes **4**·3MeCN and **5**·2MeCN

	4·3MeCN	**5**·2MeCN
Formula	$C_{62}H_{67}Cl_3Fe_2N_{17}O_{16}$	$C_{65}H_{67}Cl_3Fe_2N_{16}O_{16}$
M	1523.4	1545.4
Crystal system	Triclinic	Monoclinic
Space group	$P\bar{1}$	$P2_1/n$
a/Å	14.089(3)	25.760(6)
b/Å	16.377(3)	14.697(3)
c/Å	16.686(4)	19.350(4)
α/°	86.06(2)	90.00(0)
β/°	80.66(2)	90.42(2)
γ/°	74.19(1)	90.00(0)
U/Å^3	3654(1)	7326(3)
D_c/g cm^{-3}	1.39	1.40
Z	2	4
μ/cm^{-1}	5.75	5.77
F(000)	1578	3200
h, k, l ranges	0–16, 0–18, −18 to 18	0–16, 0–21, −28 to 28
2θ range/°	2–45	2–45
No. of reflections collected	10 283	10 561
No. of reflections for refinement [$I > 4\sigma(I)$]	5809	6012
No. of variables	930	964
R	0.0801	0.0869
R'	0.0669	0.0736

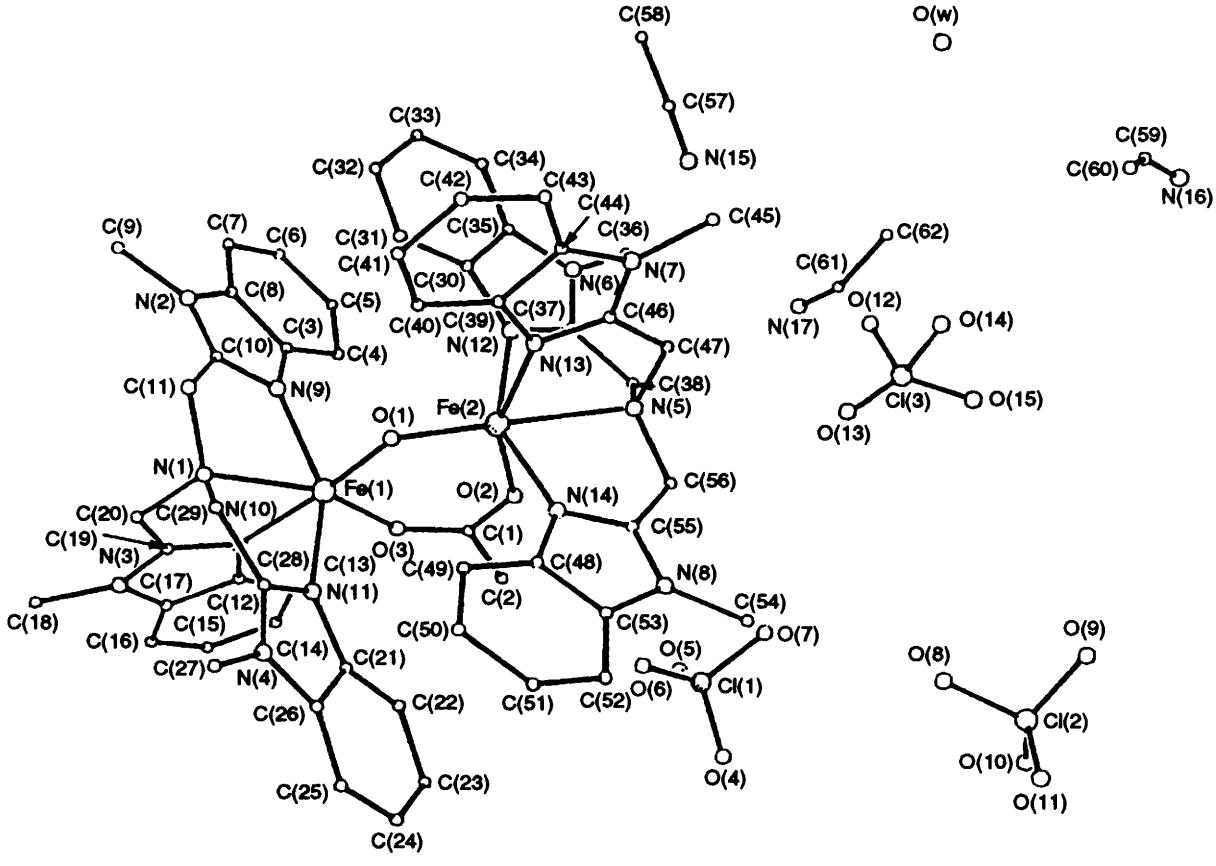

Fig. 1 Perspective view of the complex **4**·3MeCN showing the atomic numbering scheme

Crystal Structures.—The structures of complexes **4**·3MeCN and **5**·2MeCN consist of a μ-oxo-μ-carboxylato-diiron core $[Fe_2O(O_2CR)L^2_2]^{3+}$ (R = Me or Ph), three perchlorate counter anions, one water molecule, and three acetonitrile solvate molecules for the former and two for the latter. The final atomic positional coordinates are listed in Table 2, selected bond distances and angles in Table 3. Figs. 1 and 2 show perspective views of the **4**·3MeCN and **5**·2MeCN molecules with atom numbering. The complexes exhibit similar geometries. Each Fe atom has an N_4O_2 donor set in a distorted octahedron with N-donors from the tripodal ligand and O-donors from a bridging oxide and a bridging bidentate carboxylate. The Fe–N (benzimidazole) bond lengths (average 2.123 Å for **4**·3MeCN and 2.115 Å for **5**·2MeCN) are longer than those found in $[L^4FeOFeCl_3]^+$ [L^4 = *N*,*N*,*N*′-tris(benzimidazol-2-ylmethyl)-*N*′-(2-hydroxyethyl)ethane-1,2-diamine] (2.094 Å)[13a] and $[Fe_2O(O_2CPh)_2L^5_2]^{2+}$ [L^5 = bis(benzimidazol-2-yl)amine] (2.108 Å),[9] but shorter than those found in $[Fe_4O_2(O_2CPh)_2L^6_2]^{4+}$ {L^6 = 1,3-bis[bis-(benzimidazol-2-ylmethyl)amino]propan-2-ol} (2.185 Å)[26]

Table 2 Atomic coordinates ($\times 10^4$)

Atom	*x*	*y*	*z*	Atom	*x*	*y*	*z*
Complex **4**·3MeCN							
Fe(1)	4 252(1)	−2 784(1)	2 281(1)	C(17)	5 852(7)	−5 004(5)	759(6)
Fe(2)	3 397(1)	−780(1)	2 706(1)	C(18)	5 733(9)	−6 220(6)	1 780(7)
Cl(1)	6 822(2)	640(2)	851(2)	C(19)	5 018(7)	−4 641(5)	1 984(5)
Cl(2)	6 860(3)	3 595(2)	3 954(2)	C(20)	4 567(7)	−4 724(5)	2 833(5)
Cl(3)	2 787(3)	3 451(2)	3 178(2)	C(21)	6 425(7)	−2 954(6)	2 882(6)
N(1)	4 005(5)	−3 871(4)	3 178(4)	C(22)	6 956(9)	−2 575(8)	2 291(8)
N(2)	1 751(5)	−3 712(4)	2 313(4)	C(23)	7 889(13)	−2 501(13)	2 434(13)
N(3)	5 529(6)	−5 324(4)	1 526(5)	C(24)	8 232(12)	−2 818(11)	3 140(14)
N(4)	6 113(6)	−3 602(4)	4 070(5)	C(25)	7 725(10)	−3 201(8)	3 746(10)
N(5)	3 180(5)	686(4)	2 319(4)	C(26)	6 802(7)	−3 265(6)	3 603(6)
N(6)	1 342(6)	442(4)	1 168(4)	C(27)	6 185(10)	−3 976(7)	4 886(7)
N(7)	1 438(5)	1 017(4)	4 280(4)	C(28)	5 358(7)	−3 489(5)	3 649(5)
N(8)	5 381(5)	489(5)	3 300(4)	C(29)	4 400(8)	−3 725(6)	3 917(5)
N(9)	2 923(5)	−3 033(4)	2 030(4)	C(30)	1 329(7)	−667(5)	2 024(5)
N(10)	4 977(5)	−3 921(4)	1 580(4)	C(31)	970(7)	−1 281(6)	2 464(6)
N(11)	5 489(5)	−3 104(4)	2 936(4)	C(32)	56(9)	−1 356(8)	2 311(8)
N(12)	2 176(5)	−399(4)	2 057(4)	C(33)	−451(8)	−837(7)	1 742(8)
N(13)	2 393(5)	−162(4)	3 678(4)	C(34)	−102(8)	−227(7)	1 309(7)
N(14)	4 470(5)	−388(4)	3 203(4)	C(35)	803(7)	−136(6)	1 457(6)
O(1)	3 577(4)	−1 888(3)	2 915(3)	C(36)	1 076(10)	1 098(7)	542(6)
O(2)	4 338(4)	−838(3)	1 621(3)	C(37)	2 129(7)	263(5)	1 558(5)
O(3)	4 785(5)	−2 197(3)	1 328(3)	C(38)	2 858(7)	770(5)	1 513(5)
O(4)	7 786(7)	658(8)	846(9)	C(39)	1 928(6)	−394(5)	4 438(5)
O(5)	6 751(8)	499(8)	61(5)	C(40)	1 984(7)	−1 170(6)	4 822(5)
O(6)	6 542(10)	54(7)	1 406(6)	C(41)	1 432(8)	−1 190(6)	5 589(6)
O(7)	6 158(9)	1 455(7)	1 029(6)	C(42)	842(8)	−450(7)	5 955(6)
O(8)	6 416(11)	2 924(8)	4 027(12)	C(43)	786(7)	322(7)	5 588(6)
O(9)	6 106(11)	4 296(7)	4 066(8)	C(44)	1 326(6)	354(5)	4 815(5)
O(10)	7 459(13)	3 555(14)	3 238(7)	C(45)	955(7)	1 910(5)	4 421(6)
O(11)	7 431(8)	3 483(8)	4 573(6)	C(46)	2 084(6)	664(5)	3 630(5)
O(12)	2 135(19)	3 329(10)	2 783(12)	C(47)	2 414(7)	1 194(5)	2 928(5)
O(13)	3 247(13)	2 790(6)	3 587(10)	C(48)	5 067(6)	−720(5)	3 796(5)
O(14)	2 197(16)	3 899(19)	3 821(11)	C(49)	5 099(8)	−1 421(6)	4 307(6)
O(15)	3 081(11)	4 104(7)	2 937(14)	C(50)	5 762(9)	−1 584(7)	4 864(7)
C(1)	4 826(6)	−1 439(5)	1 182(5)	C(51)	6 373(9)	−1 029(10)	4 888(8)
C(2)	5 504(7)	−1 259(6)	445(5)	C(52)	6 348(9)	−335(11)	4 397(8)
C(3)	2 379(7)	−2 889(5)	1 392(5)	C(53)	5 655(7)	−169(6)	3 847(6)
C(4)	2 440(8)	−2 393(6)	685(6)	C(54)	5 812(9)	1 221(8)	3 149(7)
C(5)	1 748(11)	−2 365(7)	171(7)	C(55)	4 678(7)	331(6)	2 927(5)
C(6)	1 040(11)	−2 808(7)	347(8)	C(56)	4 159(7)	858(6)	2 287(6)
C(7)	950(9)	−32 788(6)	1 032(7)	C(57)	−734(15)	1 935(10)	2 329(8)
C(8)	1 636(7)	−3 318(5)	1 567(5)	C(58)	−1 683(12)	1 860(12)	2 197(9)
C(9)	1 117(9)	−4 248(7)	2 728(8)	C(59)	313(19)	6 069(10)	5 097(14)
C(10)	2 525(6)	−3 522(5)	2 561(5)	C(60)	508(16)	5 721(14)	5 910(18)
C(11)	2 917(7)	−3 787(6)	3 341(5)	C(61)	1 541(26)	3 362(21)	486(19)
C(12)	5 495(7)	−4 127(5)	793(5)	C(62)	866(29)	3 994(24)	973(25)
C(13)	5 670(7)	−3 631(6)	117(5)	N(15)	13(10)	1 966(9)	2 461(8)
C(14)	6 189(8)	−4 011(7)	−578(7)	N(16)	478(16)	6 475(13)	4 526(12)
C(15)	6 544(9)	−4 882(9)	−615(7)	N(17)	1 771(28)	2 924(21)	−90(19)
C(16)	6 400(9)	−5 389(7)	27(9)	O(w)	−1 661(27)	5 100(23)	1 713(22)
Complex **5**·2MeCN							
Fe(1)	9 238(1)	1 821(1)	3 710(1)	C(18)	7 283(5)	1 731(4)	3 298(6)
Fe(2)	9 679(1)	1 757(1)	1 586(1)	C(19)	6 546(5)	1 707(5)	3 272(8)
Cl(1)	4 136(2)	1 770(1)	2 632(2)	C(20)	6 167(5)	1 779(5)	4 061(8)
Cl(2)	8 383(2)	999(1)	1 838(2)	C(21)	6 475(5)	1 886(5)	4 866(7)
Cl(3)	1 910(1)	2 247(2)	6 068(2)	C(22)	7 190(4)	1 919(4)	4 896(6)
N(1)	9 562(3)	1 922(3)	5 254(4)	C(23)	7 482(6)	2 122(5)	6 532(6)
N(2)	9 386(4)	515(3)	5 428(4)	C(24)	8 293(4)	1 991(3)	5 225(6)
N(3)	7 651(4)	2 016(3)	5 589(5)	C(25)	8 935(4)	2 077(4)	5 769(6)
N(4)	9 868(4)	3 275(3)	4 678(5)	C(26)	9 151(4)	3 077(4)	3 539(6)
N(5)	9 031(3)	2 086(3)	411(4)	C(27)	8 670(4)	3 147(4)	2 849(6)
N(6)	8 154(4)	832(4)	486(5)	C(28)	8 522(6)	3 652(5)	2 622(7)
N(7)	10 604(4)	1 912(3)	−1 007(4)	C(29)	8 836(6)	4 061(5)	3 048(9)
N(8)	9 758(4)	3 366(3)	1 073(5)	C(30)	9 312(6)	3 995(4)	3 737(8)
N(9)	9 233(3)	1 061(3)	4 277(4)	C(31)	9 459(5)	3 497(4)	3 980(6)
N(10)	8 282(3)	1 888(3)	4 345(4)	C(32)	10 321(6)	3 565(5)	5 304(8)
N(11)	9 380(3)	2 617(3)	3 935(4)	C(33)	9 797(4)	2 761(4)	4 623(5)
N(12)	9 169(3)	1 126(3)	970(5)	C(34)	10 068(4)	2 353(4)	5 254(6)
N(13)	10 403(3)	1 781(3)	471(4)	C(35)	9 182(6)	585(4)	996(6)
N(14)	9 913(3)	2 567(3)	1 643(4)	C(36)	9 720(7)	246(5)	1 240(7)

Table 2 (*continued*)

Atom	*x*	*y*	*z*	Atom	*x*	*y*	*z*
Complex **5**·2MeCN							
O(1)	9 068(2)	1 796(2)	2 510(3)	C(37)	9 579(11)	−274(5)	1 167(9)
O(2)	10 312(3)	1 691(2)	3 631(3)	C(38)	8 918(13)	−437(6)	873(10)
O(3)	10 405(3)	1 365(2)	2 233(3)	C(39)	8 403(8)	−128(5)	621(9)
O(4)	4 261(9)	1 585(9)	3 390(10)	C(40)	8 555(7)	397(4)	698(7)
O(5)	3 829(9)	1 598(9)	1 963(13)	C(41)	7 422(6)	844(6)	166(9)
O(6)	4 782(8)	1 910(7)	2 301(12)	C(42)	8 561(5)	1 246(4)	659(6)
O(7)	3 769(10)	2 219(7)	8 860(13)	C(43)	8 371(4)	1 807(4)	485(6)
O(8)	8 190(5)	953(4)	6 924(6)	C(44)	11 108(4)	1 739(3)	316(5)
O(9)	7 992(4)	1 360(4)	8 352(5)	C(45)	11 656(4)	1 638(4)	911(5)
O(10)	9 069(5)	1 213(5)	7 778(8)	C(46)	12 309(6)	1 615(5)	547(8)
O(11)	8 493(8)	530(5)	8 248(7)	C(47)	12 437(5)	1 692(5)	−370(8)
O(12)	1 490(10)	2 721(8)	6 307(17)	C(48)	11 909(5)	1 805(4)	−960(7)
O(13)	1 431(4)	1 842(4)	6 160(5)	C(49)	11 243(4)	1 817(4)	−604(5)
O(14)	2 009(8)	2 414(5)	5 240(7)	C(50)	10 478(6)	2 005(5)	−1 979(6)
O(15)	2 353(5)	2 335(5)	6 748(7)	C(51)	10 128(4)	1 887(4)	−330(6)
C(1)	10 625(4)	1 430(4)	3 037(5)	C(52)	9 375(4)	1 953(4)	−470(5)
C(2)	11 309(4)	1 191(4)	3 264(6)	C(53)	10 368(4)	2 902(4)	2 075(6)
C(3)	11 530(5)	755(4)	2 771(7)	C(54)	10 863(4)	2 815(4)	2 761(7)
C(4)	12 183(7)	551(5)	2 980(10)	C(55)	11 229(5)	3 232(5)	3 056(7)
C(5)	12 607(6)	789(5)	3 626(10)	C(56)	11 138(6)	3 715(4)	2 713(9)
C(6)	12 374(6)	1 195(6)	4 073(9)	C(57)	10 670(6)	3 820(4)	2 041(8)
C(7)	11 714(5)	1 410(5)	3 912(7)	C(58)	10 280(5)	3 400(4)	1 737(7)
C(8)	8 934(4)	586(4)	4 045(6)	C(59)	9 466(7)	3 784(5)	529(8)
C(9)	8 572(5)	437(4)	3 263(7)	C(60)	9 565(5)	2 855(4)	1 070(6)
C(10)	8 338(6)	−67(4)	3 240(7)	C(61)	8 957(5)	2 658(4)	525(6)
C(11)	8 438(6)	−415(5)	3 975(8)	C(62)	6 502(11)	257(11)	5 074(19)
C(12)	8 775(6)	−261(4)	4 746(7)	C(63)	7 142(8)	533(7)	5 134(13)
C(13)	9 023(5)	244(4)	4 769(6)	C(64)	3 874(22)	100(17)	969(25)
C(14)	9 599(6)	302(4)	5 321(6)	C(65)	3 342(25)	501(20)	1 037(33)
C(15)	9 494(4)	996(4)	5 105(5)	N(15)	5 952(11)	109(12)	5 334(22)
C(16)	9 858(5)	1 428(4)	5 567(6)	N(16)	4 205(21)	−162(16)	428(30)
C(17)	7 574(4)	1 837(4)	4 113(5)	O(w)	5 587(22)	475(18)	2 500(30)

and $[Fe_2OL^1{}_2Cl_2]^{2+}$ (2.145 Å).[15b] The Fe–N (tertiary amine) bond lengths in **4**·3MeCN and **5**·2MeCN range from 2.289(7) to 2.393(6) Å which are significantly longer than the Fe–N (benzimidazole) bond lengths. In general imidazole ligands are good π donors compared to amine and pyridine and therefore have shorter metal–ligand bond lengths.[27] The Fe(1)–N(10) (benzimidazole) [2.180(6) Å] and Fe(2)–N(5) (tertiary amine) [2.393(6)(13) Å] in **4**·3MeCN, and Fe(2)–N(13) (benzimidazole) [2.165(6) Å] and Fe(1)–N(1) (tertiary amine) [2.365(6) Å] in **5**·2MeCN are markedly longer than the other corresponding bond lengths. This is because these bonds are *trans* to the bridging oxo group. A similar *trans* influence is observed for the imidazole ligands bonded to the bridging oxo group in azidomethaemerythrin.[2,3] Fe–O(oxo) distances in **4**·3MeCN and **5**·2MeCN [1.780(5)–1.817(4) Å] are longer than those observed in methaemerythrin and azidometmyohaemerythrin with average Fe–O (oxo) 1.78 Å,[1b] while the Fe–O–Fe angles [129.8(3)° for **4**·3MeCN and 128.6(3)° for **5**·2MeCN] fall within the range 127–135° found in the above μ-oxo-diiron proteins. The Fe···Fe separations for **4**·3MeCN and **5**·2MeCN are 3.258 and 3.246 Å respectively, comparable to those (3.21–3.25 Å) found in methaemerythrin.[1b] However, in the previously reported μ-oxo-bis(carboxylato)-diiron(III) complexes the separations (3.12 ± 0.05 Å) are significantly shorter.[1b]

The interesting feature of complexes **4**·3MeCN and **5**·2MeCN, also observed in μ-oxo-μ-carboxylato-diiron complexes with tris(2-pyridylmethyl)amine (tpma),[11a] is the inequivalence of the two iron sites at which the two ligands have two different orientations. On one Fe the benzimidazole nitrogen atom is *trans* to the oxo-bridge, while on the other the tertiary amine nitrogen atom is *trans* to the oxo-bridge. Consequently, this results in differences between the Fe(1)– and Fe(2)–O (oxo), –N (amine) and –N (benzimidazole) bond lengths (see Table 3). For example, the Fe–O (oxide) bonds are inequivalent at 1.817(4) and 1.780(5) Å for **4**·3MeCN and 1.792(5) and 1.810(5) Å for **5**·2MeCN. A similar asymmetry is found for the azidometmyohaemerythrin[Fe–O (oxo) 1.80 and 1.77 Å] and azidomethaemerythrin (1.89 and 1.64 Å).[1b] In addition, in complex **4**·3MeCN the carboxylate group bridges the two Fe atoms in a very asymmetric fashion as a result of different *trans* ligands with Δ[Fe–O (carboxylate)] = 0.10 ± 0.01 Å which lies at the high end of the range found in azidometmyohaemerythrin and azidomethaemerythrin {Δ-[Fe–O(carboxylate)] = 0.04–0.11 Å}.[1b] The same behaviour was observed for complex **5**·2MeCN with Δ[Fe–O(carboxylate)] = 0.04 ± 0.01 Å. Previous synthetic μ-oxo-bis(μ-carboxylato)-diiron complexes have generally some effective symmetry element such as a two-fold axis or a plane which relates the two halves of the molecules to give two essentially equivalent iron sites. Thus, the asymmetry of the iron sites in μ-oxo-diiron proteins is not modelled by those complexes. In **4**·3MeCN and **5**·2MeCN, the core dimensions, including the inequivalence of two iron sites, match well with those found in μ-oxo-diiron proteins (Table 4). It can be also seen that **4**·3MeCN and **5**·2MeCN exhibit, like asymmetric $[Fe_2O(O_2CMe)(tpma)_2]^{3+}$,[11a] Fe···Fe and Fe–O (oxo) distances and Fe–O–Fe angles which more closely mimic those of azidomethaemerythrin than do those of the symmetric model $[Fe_2O(O_2CMe)_2\{HB(pz)_3\}_2]$ (pz = pyrazolyl).

^{1}H *NMR Spectroscopy*.—In order to elucidate the structures of the complexes in solution, the ^{1}H NMR spectra of complexes **1** and **4** were recorded in CD_3CN (Fig. 3). It can be seen that all of the signals appear within the range δ 0–35, indicating the strong antiferromagnetic coupling between the iron centres. Comparison of the spectra indicates that the peaks in the range δ 4.5–5.5 arise from the benzimidazole N–CH_3 protons for the L^2 ligand.[28] The presence of three peaks at δ 5.5, 4.8 and

Table 3 Selected bond lengths (Å) and angles (°)

Complex **4**·3MeCN			
Fe(1)–N(1)	2.309(6)	Fe(1)–N(9)	2.131(8)
Fe(1)–N(10)	2.180(6)	Fe(1)–N(11)	2.132(8)
Fe(1)–O(1)	1.817(4)	Fe(1)–O(3)	1.953(6)
Fe(2)–N(5)	2.393(6)	Fe(2)–N(12)	2.109(7)
Fe(2)–N(13)	2.088(6)	Fe(2)–N(14)	2.096(8)
Fe(2)–O(1)	1.780(5)	Fe(2)–O(2)	2.055(5)
N(1)–Fe(1)–N(9)	75.0(2)	N(1)–Fe(1)–N(10)	76.7(2)
N(9)–Fe(1)–N(10)	83.2(3)	N(1)–Fe(1)–N(11)	74.2(2)
N(9)–Fe(1)–N(11)	149.1(3)	N(10)–Fe(1)–N(11)	87.5(3)
N(1)–Fe(1)–O(1)	98.9(2)	N(9)–Fe(1)–O(1)	93.4(2)
N(10)–Fe(1)–O(1)	175.0(3)	N(11)–Fe(1)–O(1)	93.5(2)
N(1)–Fe(1)–O(3)	160.2(2)	N(9)–Fe(1)–O(3)	107.5(3)
N(10)–Fe(1)–O(3)	84.0(2)	N(11)–Fe(1)–O(3)	100.7(3)
O(1)–Fe(1)–O(3)	100.5(2)	N(5)–Fe(2)–N(12)	71.8(3)
N(5)–Fe(2)–N(13)	77.3(2)	N(12)–Fe(2)–N(13)	85.0(2)
N(5)–Fe(2)–N(14)	74.0(2)	N(12)–Fe(2)–N(14)	145.7(3)
N(13)–Fe(2)–N(14)	85.2(3)	N(5)–Fe(2)–O(1)	175.7(2)
N(12)–Fe(2)–O(1)	106.2(3)	N(13)–Fe(2)–O(1)	106.5(2)
N(14)–Fe(2)–O(1)	108.2(3)	N(5)–Fe(2)–O(2)	77.5(2)
N(12)–Fe(2)–O(2)	88.8(2)	N(13)–Fe(2)–O(2)	154.7(2)
N(14)–Fe(2)–O(2)	86.2(2)	O(1)–Fe(2)–O(2)	98.8(2)
Fe(1)–O(1)–Fe(2)	129.8(3)	Fe(2)–O(2)–C(1)	132.5(5)
Complex **5**·2MeCN			
Fe(1)–N(1)	2.365(6)	Fe(1)–N(9)	2.128(7)
Fe(1)–N(10)	2.085(6)	Fe(1)–N(11)	2.096(7)
Fe(1)–O(1)	1.792(5)	Fe(1)–O(2)	2.110(5)
Fe(2)–N(5)	2.289(7)	Fe(2)–N(12)	2.102(7)
Fe(2)–N(13)	2.165(6)	Fe(2)–N(14)	2.135(7)
Fe(2)–O(1)	1.810(5)	Fe(2)–O(3)	1.969(6)
N(1)–Fe(1)–N(9)	74.2(2)	N(1)–Fe(1)–N(10)	77.9(2)
N(9)–Fe(1)–N(10)	83.9(3)	N(1)–Fe(1)–N(11)	72.9(2)
N(9)–Fe(1)–N(11)	147.1(3)	N(10)–Fe(1)–N(11)	87.9(3)
N(10)–Fe(1)–O(1)	173.5(2)	N(9)–Fe(1)–O(1)	110.6(3)
N(10)–Fe(1)–O(1)	106.7(2)	N(11)–Fe(1)–O(1)	102.3(3)
N(1)–Fe(1)–O(2)	79.4(2)	N(9)–Fe(1)–O(2)	83.2(2)
N(10)–Fe(1)–O(2)	156.2(2)	N(12)–Fe(2)–N(13)	90.0(3)
O(1)–Fe(1)–O(2)	96.6(2)	N(12)–Fe(2)–N(14)	150.5(3)
N(5)–Fe(2)–N(13)	76.8(2)	N(12)–Fe(2)–N(13)	90.0(3)
N(5)–Fe(2)–N(14)	77.5(3)	N(12)–Fe(2)–N(14)	150.5(3)
N(13)–Fe(2)–N(14)	82.2(3)	N(5)–Fe(2)–O(1)	100.9(2)
N(12)–Fe(2)–O(1)	93.4(3)	N(13)–Fe(2)–O(1)	175.2(3)
N(14)–Fe(2)–O(1)	93.2(3)	N(5)–Fe(2)–O(3)	159.8(2)
N(12)–Fe(2)–O(3)	98.1(3)	N(13)–Fe(2)–O(3)	85.2(2)
N(14)–Fe(2)–O(3)	109.4(3)	O(1)–Fe(2)–O(3)	97.7(2)
Fe(1)–O(1)–Fe(2)	128.6(3)	Fe(1)–O(2)–C(1)	126.9(5)

4.5 with a area ratio of 3:2:1 respectively reflects the differences in metal–benzimidazole nitrogen bonding at the two iron sites, indicating that the solid-state structure determined by X-ray crystallography is retained in solution.[11a] In the solid state, as discussed above, **4** contains two distinct iron sites and two different orientations of L^2, suggesting that the six benzimidazole groups of the two L^2 ligands at the two iron(III) sites would have a 3:2:1 pattern. That is, the environments of three benzimidazole groups at Fe(2) are distinctly different from those of the three at Fe(1). Furthermore, the environment of the benzimidazole group *trans* to the oxo bridge at Fe(1) is also distinctly different from those of the other two *cis* to the oxo bridge[28] [see Fig. 1 and Fe(1)– or Fe(2)–N(benzimidazole) bond lengths in Table 3]. This results in the pattern observed for these N–CH_3 protons. Thus, the peak with relative intensity of 1 at δ 4.5 is assigned to the N–CH_3 protons of the benzimidazole group *trans* to the oxo bridge at Fe(1), that with relative intensity 2 is assigned to the N–CH_3 protons of the other two *cis* to the oxo bridge of Fe(1) and that with relative intensity 3 is assigned to the N–CH_3 protons of three benzimidazole groups at Fe(2). These assignments are in accord with the bond distances between the benzimidazole groups and the two iron(III) centres. The N–CH_3 protons of the benzimidazole group *trans* to the oxo bridge have the longest benzimidazole group-to-Fe(1) distance, and therefore, the smallest paramagnetic shift and the ^1H NMR signal appears at the highest field in the region of δ 4.5–5.5, while the N–CH_3 protons of the three benzimidazole groups at Fe(2) have short benzimidazole group-to-Fe(2) distances and therefore, the largest paramagnetic shift and their signal appears at lowest field.

When complex **4** dissolved in CD_3CN solution was allowed to stand for several days the ^1H NMR signals became broad and poorly resolved, probably due to exchange of the bridging carboxylate group with solvate molecules, the counter anion or crystal water molecules. In the spectrum of **1**, the broad features in the δ 17–18 region disappear when D_2O is added to a CD_3CN solution, suggesting that the peaks arise from the benzimidazole NH protons. The NH proton resonance region also contains three poorly resolved peaks at δ 17, 17.5 and 18.0, as previously observed.[15b] The inequivalence of the benzimidazole NH protons in **1** indicates that the complex contains two spectroscopically distinct iron sites in solution. It is worth pointing out that the region where the NH resonances are found for **1** is also where histidine NH resonances have been observed for azidomethaemerythrin[29] and ribonucleotide reductase.[30] The broad resonance at *ca.* δ 10 for **1** and **4** is assigned to the methyl protons of the bridging carboxylate group.[5,7,28] The relatively sharp features in the range δ 6.0–7.5 for these complexes indicate that the protons are distant from the iron centre and thus are assigned to the benzimidazole C^5 or C^6 protons, while the broad features in the range δ 11–35 may be assigned to those nearest the iron centres, such as the methylene protons and the benzimidazole C^4 protons. Although these proton resonances cannot be definitively assigned, they exhibit the complex patterns which strongly indicate the absence of any symmetric element in the μ-oxo-diiron cores.

Physical Properties.—The electronic spectra of complexes **1**–**7** (Table 5) exhibit similar features, including a strong band at *ca.* 370 nm, a shoulder near 330 nm, and a broad band at *ca.* 600 nm. The first two are attributed to the O→Fe^{III} charge-transfer transitions, while the band at *ca.* 600 nm is assigned to the d–d transition $^6A_1 \longrightarrow {}^4T_2(^4G)$. These results are qualitatively similar to those observed for related μ-oxo-diiron model complexes and μ-oxo-diiron proteins.[5a] In the IR spectra of the complexes the symmetric and antisymmetric stretching modes of the carboxylate groups occur at *ca.* 1402 and 1505 cm^{-1} respectively. The Fe–O–Fe asymmetric stretching modes are assignable at *ca.* 755 cm^{-1} as a shoulder, while the symmetric modes are tentatively assigned at *ca.* 470 cm^{-1}. The perchlorate and nitrate anions all show the expected vibrations (≈1090, 625 cm^{-1} for ClO_4^- and 1355 cm^{-1} for NO_3^-) typical of ionic perchlorate and nitrate. The bands assigned to crystal water stretching vibrations occur in the range from 3327 to 3423 cm^{-1}

The resonance-Raman spectra for complexes **2** and **4**–**6** were recorded and these data are summarized in Table 6. The dominant feature at *ca.* 475 cm^{-1} is the Fe–O–Fe symmetric stretching mode ν_{sym}(Fe–O–Fe), while the asymmetric stretching mode ν_{asym}(Fe–O–Fe) occurs in the range 748–760 cm^{-1}, typical for μ-oxo-diiron complexes.[31] The intensity ratio I_{asym}/I_{sym} for the complexes falls in the range 0.19–0.26:1, which is significantly larger than those (< 0.1:1) found for symmetrical μ-oxo-bis(μ-carboxylato)-diiron complexes,[1b] but similar to those found in the similar asymmetric μ-oxo-μ-carboxylato-diiron complex with tpma(0.18–0.33:1)[11a] and methaemerythrin halide complexes (0.18–0.30:1).[31] This shows that the inequivalence in the iron sites of the present complexes has a significant effect on the Raman spectra, as an enhancement of ν_{asym}(Fe–O–Fe) leading to a large intensity ratio I_{asym}/I_{sym}, as previously observed.[11a,13] Thus, the I_{asym}/I_{sym} ratio may serve

Table 4 Comparison of structural and physical properties

	4	5	$[Fe_2O(O_2CMe)(tpma)_2]^{3+}$ [a]	$[Fe_2O(O_2CMe)_2\{HB(pz)_3\}_2]$ [b]	Azidomethaemerythrin [c]
Fe–O (oxo)/Å	1.817(4), 1.780(5)	1.792(5), 1.810(5)	1.804(5), 1.776(4)	1.780(2), 1.788(2)	1.89, 1.64
Δ[Fe–O (oxo)]/Å	0.037	0.018	0.028	0.008	0.22
Fe–O (carboxylate)/Å	1.953(6), 2.055(5)	1.969(6), 2.110(5)	1.972(6), 2.038(6)	2.040(2), 2.041(2) 2.050(3), 2.040(2)	2.24, 2.33 2.16, 2.20
Δ[Fe–O (carboxylate)]/Å	0.102	0.041	0.066	≈0, 0.01	0.09, 0.04
Fe · · · Fe/Å	3.258	3.246	3.243	3.146	3.25
Fe–O–Fe/°	129.8(3)	128.6(3)	129.2(3)	123.6(1)	134.5
$-J$ [d]/cm^{-1}	108.22	—	114.3	121	–
ν_{sym}(Fe–O–Fe) [e]/cm^{-1}	479	478	449	528	507
ν_{asym}(Fe–O–Fe) [e]/cm^{-1}	760	752	770	751	770
δ [f]/mm s^{-1}	0.45	0.46	0.45	0.52	0.50
ΔE_Q [f]/mm s^{-1}	1.38	1.38	1.45	1.60	1.91

[a] Ref. 11*a*. [b] Ref. 5*a*. [c] Ref. 1*b*. [d] Molar susceptibility data. [e] Resonance-Raman data. [f] Mössbauer data.

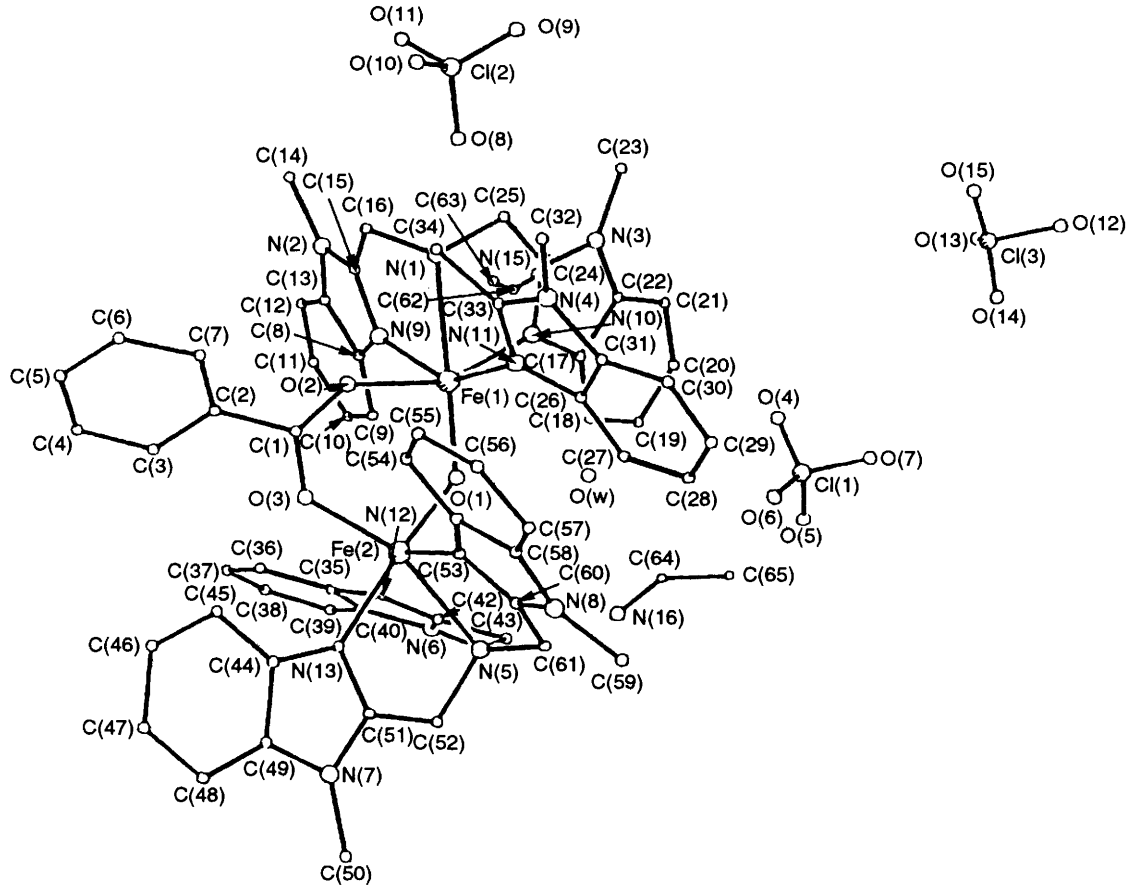

Fig. 2 Perspective view of the complex **5**·2MeCN showing the atomic numbering scheme

Table 5 Electronic and IR spectroscopic properties of the complexes

Complex	Electronic, λ_{max}/nm (ε/dm^{3}mol^{-1} cm^{-1})			IR (cm^{-1})		
				$\nu_{asym}(CO_2^-)$	$\nu_{sym}(CO_2^-)$	ν_{asym}(Fe–O–Fe)
1	333 (sh)	363 (3210)	589 (87)	1543s	1395s	755 (sh)
2	331 (sh)	372 (3224)	602 (88)	1493s	1399s	756 (sh)
3	330 (sh)	377 (3308)	606 (90)	1507s	1355s	754 (sh)
4	329 (sh)	379 (3220)	602 (91)	1505s	1423s	757 (sh)
5	330 (sh)	371 (3450)	606 (88)	1504s	1418s	760 (sh)
6	335 (sh)	375 (3302)	589 (88)	1506s	1420s	758 (sh)
7	318 (sh)	378 (3230)	607 (86)	1495vs	1402s	756 (sh)

Table 6 Mössbauer and resonance-Raman data for the complexes

Complex	Mössbauer		Resonance Raman (cm^{-1})		
	δ/mm s^{-1}	ΔE_Q/mm s^{-1}	ν_{asym}(Fe–O–Fe)	ν_{sym}(Fe–O–Fe)	I_{asym}/I_{sym} *
2	—	—	758	476	0.19
4	0.45	1.38	760	479	0.26
5	0.46	1.38	752	478	0.21
6	0.47	1.39	748	470	0.23

* Raman scattering intensity (peak area) of ν_{asym}(Fe–O–Fe) relative to that of ν_{sym}(Fe–O–Fe).

as a useful indicator of the asymmetry of dinuclear oxo iron complexes.

Solution magnetic susceptibility measurements were carried out for complexes **4** and **5** in acetonitrile using the Evans method.[32] The effective magnetic moments were determined to be 1.63 and 1.68 μ_B respectively, which are much smaller than 5.48 μ_B for high-spin mononuclear iron(III), indicating that the μ-oxo-diiron core of the complexes is retained in solution. Solid-state variable-temperature magnetic susceptibility studies have been performed for **4**. A non-linear least-squares fitting program (written in FORTRAN IV locally by Dr. Y. Kejiang) was used to fit the observed data with equation (1) under the following conditions: (*i*) fixing $g = 2$ and $N_\alpha = 0$, refining J and P gave $-J = 108.09$ cm^{-1}, $P = 3.08 \times 10^{-4}$ and $R = 2.2 \times 10^{-3}$; (*ii*) fixing $g = 2$, refining J, P and N_α gave $-J = 108.22$ cm^{-1}, $P = 3.01 \times 10^{-4}$, $N_\alpha = 1.55 \times 10^{-5}$ emu and $R = 2.08 \times 10^{-3}$. A plot of molar magnetic susceptibility (χ_m) as a function of temperature (with g fixed at 2) is shown in Fig. 4.

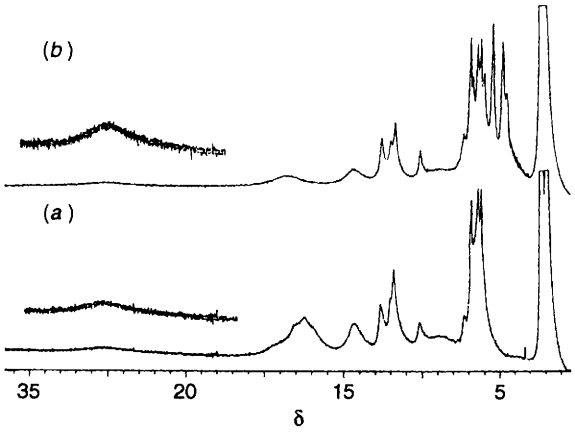

Fig. 3 Proton NMR spectra of complexes **1**(*a*) and **4**(*b*) in CD_3CN

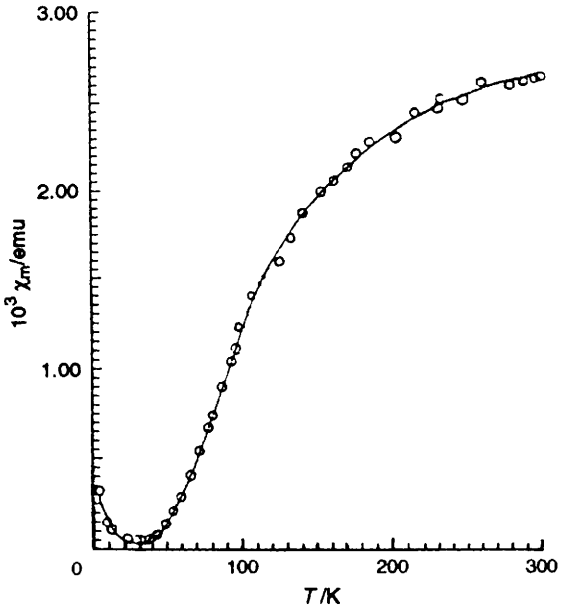

Fig. 4 Molar susceptibility (O) of complex **4** as a function of temperature. The solid line is the theoretical fit as indicated in the text

The solid line represents the calculated fit. The value of J found is similar to the range -108 to -118 cm^{-1} reported for other similar doubly bridged iron(III) complexes.[11a] However, it is somewhat less than that found for methaemerythrin ($J = -134$ cm^{-1}) and is also slightly smaller than those reported for other μ-oxo-diiron model complexes (typically -115 to -124 cm^{-1}).[1d] Considering that Kurtz[1d] has suggested that as much as 10% of the difference in J values reported from separate laboratories is due just to the different methods used in obtaining fits, the smaller J value for **4** is not interpreted as a significantly weaker antiferromagnetic coupling interaction compared to other μ-oxo-diiron model complexes. The antiferromagnetic interaction in **4** may be considered to be consistent with those in related complexes.[33]

The Mössbauer spectra for complexes **4**–**6** at room temperature were recorded and all show a slightly asymmetrical quadrupole doublet. Representative spectra are shown in Fig. 5. The isomer shifts (δ) and quadrupole splittings (ΔE_Q) are summarized in Table 6. Since the isomer shifts for high-spin mononuclear and μ-oxo-bridged dinuclear iron(III) complexes generally fall in the range 0.3–0.6 mm s^{-1},[34] the present isomer shifts (0.45–0.47 mm s^{-1}) are consistent with the presence of high-spin iron(III) ions. The isomer shift values are similar to those in azidomethaemerythrin and other dinuclear iron(III)

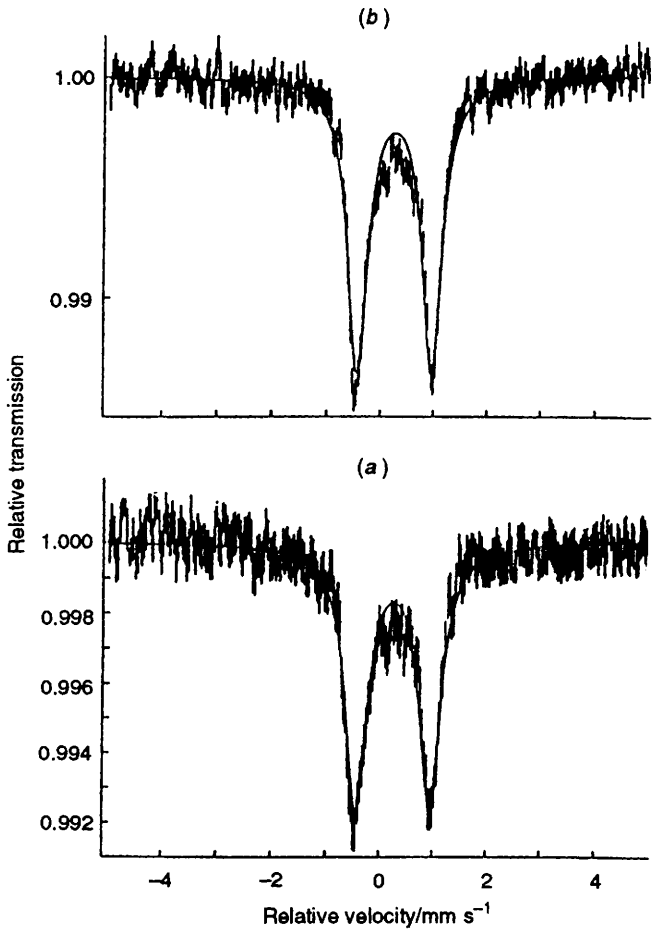

Fig. 5 Mössbauer spectra of complexes **5** (*a*) and **6** (*b*)

model complexes (Table 4). The quadrupole splittings (1.38 mm s^{-1}) are at the low end of the range 1.27–1.80 mm s^{-1} typical for oxo-bridged diiron(III),[1d] less than those found for the symmetric model complex $[Fe_2O(O_2CMe)_2\{HB(pz)_3\}_2]$ (ΔE_Q 1.6 mm s^{-1}), azidomethaemerythrin (1.91 mm s^{-1}), and also for the asymmetric complex $[Fe_2O(O_2CMe)(tpma)_2]^{3+}$ (1.45 mm s^{-1}) (Table 4), but similar to these found for other symmetric model complexes $[Fe_2O(O_2CBu^t)_2L^5]^{2+}$ (1.37 mm s^{-1})[11] and $[Fe_2O(O_2CMe)_2L^7{}_2]^{4+}$ [L^7 = *N*,*N*,*N*′,*N*′-tetrakis(2-pyridylmethyl)propane-1,3-diamine] (1.39 mm s^{-1}).[8] This comparison shows that there appears to be no correlation between the quadrupole splitting value and the asymmetry of dinuclear oxo iron complexes. The observed linewidths for **4**–**6** (full widths at half-maximum Γ = 0.460–0.499 mm s^{-1}) are significantly larger than the value of 0.310 mm s^{-1} observed for the symmetrical complex $[Fe_2O(O_2CMe)_2\{HB(pz)_3\}_2]$.[5a]

Cyclic voltammograms of complexes **2**, **4** and **6** were recorded in acetonitrile solution in the -0.5 to 1.50 V potential range *versus* SCE. As previously reported,[15b] an irreversible reduction wave is found at 0.03 V for **2**, -0.02 V for **4** and -0.05 V for **6**, and irreversible oxidation waves at 0.75, 0.79 and 0.66 V respectively, which may be assigned to $Fe^{III}Fe^{III}$–$Fe^{III}Fe^{II}$ reduction and $Fe^{III}Fe^{IV}$–$Fe^{III}Fe^{IV}$ oxidation, respectively. In addition, **4** and **6** also exhibit an oxidation wave at 1.20 and 1.05 V respectively. From Fig. 6 it is seen that for all reduction and oxidation waves there are no corresponding coupled oxidation and reduction waves. An increase in the scan rate to 800 mV s^{-1} still failed to produce such waves, indicating that all the reduction and oxidation processes are completely irreversible. The completely irreversible redox behaviour suggests that these reduction and oxidation processes probably involve reductive and oxidative decomposition of the complexes as observed

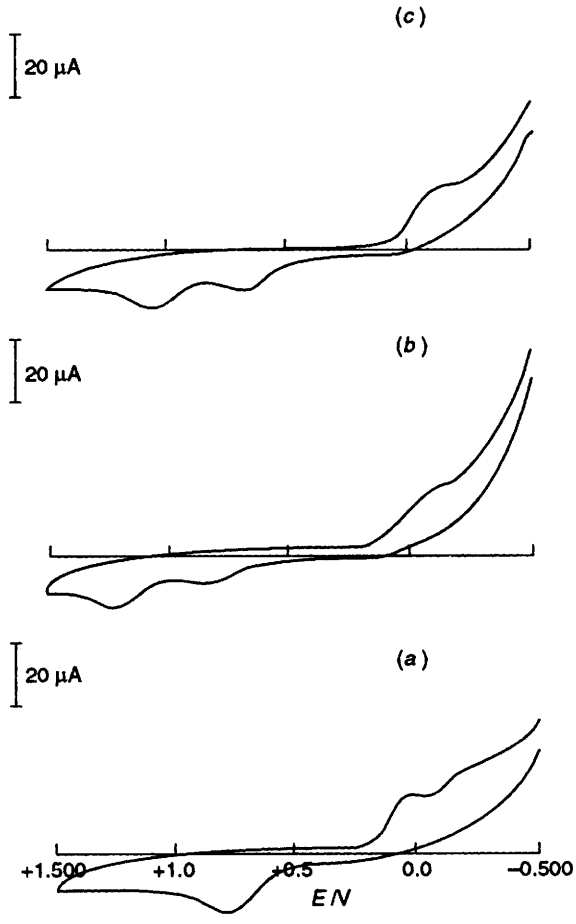

Fig. 6 Cyclic voltammograms of complexes **2** (*a*), **4** (*b*) and **6** (*c*) in MeCN at 25 °C, scan rate 0.2 V s^{-1}

previously for a symmetric μ-oxo-diiron complex.[5a] However, this is different from the behaviour of haemerythrin and asymmetric oxo-bridged tpma diiron complexes which present reversible couples at E_1 −0.31 to 0.18 V,[35] indicating that the present complexes are less stable in the cyclic voltammetric time-scale.

For comparison, some physicochemical properties of **4**, **5**, representative symmetric and asymmetric μ-oxo-diiron complexes and azidomethaemerythrin are listed in Table 4. Together with the above discussion, it can be seen that **4** and **5** exhibit physicochemical properties, such as electronic features (Table 5), Mössbauer parameters and magnetic properties, similar to those of most previously reported symmetric μ-oxo-diiron complexes. This shows that the inequivalence of the iron environments in **4** and **5** has no apparent significant effect on these physicochemical properties. However, the inequivalence is strongly reflected in the ^{1}H NMR and resonance-Raman properties of the complexes. In the ^{1}H NMR spectra the relative intensities and multiplicity of peaks associated with a particular type of protons emphasize the absence of any symmetry in complexes **1** and **4**. In the resonance-Raman spectra the inequivalence of the iron environments in **2** and **4**–**6** produces enhanced intensities for ν_{asym}(Fe–O–Fe) leading to large I_{asym}/I_{sym} values (0.19–0.26) which are significantly larger than those found for the complexes with two-fold symmetry, but match well with those found for the μ-oxo-diiron proteins. Finally, the irreversible redox behaviour of **2** and **4**–**6** is quite unlike that of haemerythrin.

Acknowledgements

This research was supported by a grant from the National Natural Science Foundation of China. We also thank Dr. Y. Cui for recording the NMR spectra, Dr. X. Dang for recording cyclic voltammograms and Miss L. Xi for preparing the manuscript.

References

1 (*a*) S. J. Lippard, *Angew. Chem., Int. Ed. Engl.*, 1988, **17**, 344; (*b*) L. Que, jun. and A. E. True, *Prog. Inorg. Chem.*, 1990, **38**, 97 and refs. therein; (*c*) J. Sanders-Loehr, in *Iron Carriers and Iron Proteins*, ed. T. M. Loehr, VCH, New York, 1989, pp. 373–466; (*d*) D. M. Kurtz, jun., *Chem. Rev.*, 1990, **90**, 585.
2 R. E. Stenkamp, L. C. Siekev and L. H, Jensen, *J. Am. Chem. Soc.*, 1984, **106**, 618; S. Sheriff, W. A. Hendrickson and J. C. Smith, *J. Mol. Biol.*, 1987, **197**, 273.
3 P. Nordlund, B.-M. Sjöberg and H. Eklund, *Nature (London)*, 1990, **345**, 593
4 A. C. Rosenzwerg, C. A. Frederick, S. J. Lippard and P. Nordlund, *Nature (London)*, 1993, **366**, 537.
5 (*a*) W. H. Armstrong, A. Spool, G. C. Papaefthymiou, R. B. Frankel and S. J. Lippard, *J. Am. Chem. Soc.*, 1984, **106**, 3653; (*b*) W. H. Armstrong and S. J. Lippard, *J. Am. Chem. Soc.*, 1984, **106**, 4632.
6 K. Wieghardt, K. Pohl and W. Gebert, *Angew. Chem., Int. Ed. Engl.*, 1983, **22**, 727.
7 J. R. Hartman, R. Rardin, P. Chaudhuri, K. Pohl, K. Wieghardt, B. Nuber, J. Weiss, G. C. Papaefthymiou, R. B. Frankel and S. J. Lippard, *J. Am. Chem. Soc.*, 1987, **109**, 7387.
8 H. Toftlund, K. S. Murray, P. R. Zwack, L. F. Taylor and O. P. Anderson, *J. Chem. Soc., Chem., Commun.*, 1986, 19.
9 P. Gomeze-Romero, N. Casan-Pastor, A. Ben-Hassein and G. B. Jameson, *J. Am. Chem. Soc.*, 1988, **110**, 1988.
10 H. Admas, N. A. Bailey, J. D. Crame, D. E. Fenton, J. M. Latour and J. M. Williams, *J. Chem. Soc., Dalton Trans.*, 1990, 1727.
11 (*a*) R. E. Norman S. Yan, L. Que, jun., G. Backes, L. Ling, J. Sander-Loehr, J. H. Zhang and C. J. O'Conner, *J. Am. Chem. Soc.*, 1990, **112**, 1554; (*b*) R. E. Norman, R. C. Holz, S. Menage, C. J. O'Connor, J. H. Zhang and L. Que, jun., *Inorg. Chem*, 1990, **29**, 4629.
12 B. Mauerer, J. Crame, J. Schuler, K. Schuler, K. Wieghardt and B. Nuber, *Angew. Chem., Int. Ed. Engl.*, 1993, **32**, 289; W. B. Tolman, A. Bino and S. J. Lippard. *J. Am. Chem. Soc.*, 1989, **111**, 8522.
13 (*a*) P. Gómez-Romero, E. H. Witten, W. M. Reiff, G. Backes, J. Sander-Loehr and G. B. Jameson, *J. Am. Chem. Soc.*, 1989, **111**, 9039; (*b*) P. Gómez-Romero, E. H. Witten, W. M. Reiff and G. B. Jameson, *Inorg. Chem.*, 1990, **29**, 2511.
14 S. Wang, Q. Luo, X. Zhou and Z. Zeng, *Polyhedron*, 1993, **12**, 1930; S. Wang, Y. Cui, R. Tan, Q. Luo, J. Shi and Q. Wu, *Polyhedron*, 1994, **13**, 1661; S. Wang, Y. Zhu, Y. Cui, L. Wang and Q. Luo, *J. Chem. Soc., Dalton Trans.*, 1994, 2523; S. Wang and Q. Luo, unpublished work.
15 (*a*) Y. Nishida, M. Nasu and T. Tokii, *Inorg. Chim. Acta*, 1990, **169**, 143; (*b*) R. M. Buchanan, R. J. O'Brien and J. F. Richardson, *Inorg. Chim. Acta*, 1993, **214**, 33.
16 L. K. Thompson, B. S. Ramaswamy and E. A. Seymour, *Can. J. Chem.*, 1977, **55**, 878; H. M. J. Hendriks, P. J. M. M. Bikes, G. C. Verschoor and J. Reedijk, *J. Chem. Soc., Dalton Trans.*, 1982, 623.
17 H. Baranska A. Labudzinska and J. Terpinski, *Laser Raman Spectrometry. Analytical Application*, Ellis Horwood, Chichester, 1987, pp. 161–163.
18 R. L. Cardin, *Magnetochemistry*, Springer, Berlin, 1986, pp. 3 and 64.
19 A. C. T. North, D. C. Phillips and F. S. Mathews, *Acta Crystallogr., Sect. A*, 1968, **24**, 351.
20 *International Tables for X-Ray Crystallography*, Kynoch Press, Birmingham, 1974, Vol. 4.
21 G. M. Sheldrick, SHELXTL, System for Crystal Structure Solution, Revision 5.1, University of Göttingen, 1986.
22 K. Wieghardt, K. Phol and D. Venture, *Angew. Chem., Int. Ed. Engl.*, 1985, **24**, 392.
23 A. Spool, I. D. Williams and S. J. Lippard, *Inorg. Chem.*, 1985, **24**, 2156.
24 W. H. Armstrong and S. J. Lippard, *J. Am. Chem. Soc.*, 1985, **107**, 3730.
25 S. Bruke, K. Wieghardt, B. Nuber and J. Weiss, *Inorg. Chem.*, 1989, **28**, 1414.
26 Q. Chen, J. B. Lynch, P. Gómez-Romero, A. Ben-Hussein, G. B. Jameson, C. O'Conner and L. Que, jun., *Inorg. Chem.*, 1988, **27**, 2673.
27 C. M. Jones, C. R. Johnson, S. A. Asher and R. R. Shepard, *J. Am. Chem. Soc.*, 1985, **107**, 3772.

28 F.-J. Wu and D. M. Kurtz, jun., *J. Am. Chem. Soc.*, 1989, **111**, 6563.
29 M. J. Marroney, D. M. Kurtz, jun., J. M. Nocek, L. Pearce and L. Que, jun., *J. Am. Chem. Soc.*, 1986, **108**, 6871.
30 M. Sahlin, A. Ehrenberg, A. Graslund and B.-M. Sjoberg, *J. Biol. Chem.*, 1986, **261**, 2778.
31 J. Sanders-Loehr, W. D. Wheeler, A. K. Shiemke, B. A. Averill and T. M. Loehr, *J. Am. Chem. Soc.*, 1989, **111**, 8084.
32 D. F. Evans, *J. Chem. Soc.*, 1958, 2003.
33 S. M. Gorun and S. J. Lippard, *Inorg. Chem.*, 1991, **30**, 1625.
34 T. C. Gibb and N. N. Greenwood, in *Mössbauer Spectroscopy*, Chapman and Hall, London, 1971, pp. 148–164.
35 R. C. Holz, T. E. Elgren, L. L. Pearce, J. H. Zhang, J. O'Connor and L. Que, jun., *Inorg. Chem.*, 1993, **32**, 5844.

Received 22*nd November* 1994; *Paper* 4/07109C